Higgs boson production and couplings with the ATLAS detector

Fernando Barreiro[1],

[1] Universidad Autónoma de Madrid, Madrid, Spain

I briefly review the status of Higgs boson production and couplings with the ATLAS detector at the LHC.

1 Introduction

The Higgs boson is the last missing piece in the Standard model. The Higgs boson is necessary to tame the singularities appearing in the amplitudes for elastic longitudinally polarized W_L and Z_L's as well as to avoid infinities in loops involving them. With the Higgs, the calculability of gauge theories is recovered, and for that it is necessary that the tree level Higgs boson couplings to fermions and gauge bosons take precise values, namely: a) $H \to WW, ZZ : gM_W, \frac{gM_Z}{cos\theta_W}$ and b)$H \to f\bar{f} : \frac{gM_f}{2M_W}$.

Without a Higgs boson the validity of the Standard Model would extend up to scales of the order of 1 TeV. With a light Higgs i.e. m_H in the range between $100 - 170$ GeV, the Standard Model can make consistent predictions up to scales close to the Planck scale i.e. 10^{19} GeV.

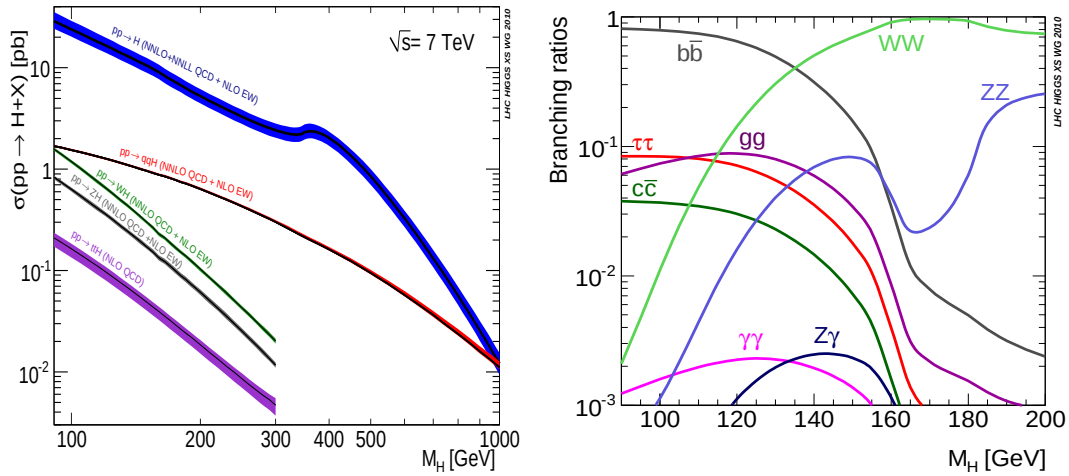

Figure 1: The cross sections for Higgs production (left) via $ggF - VBF - (W,Z)H - (t\bar{t})H$ from top to bottom, and the Higgs boson branching ratios (right) in the SM.

In $p-p$ collisions at 7 TeV, the production cross-sections for a Higgs boson with a mass in

the range 100 GeV to 1 TeV are shown on the left hand side of Fig. 1. Clearly, the dominant production process is gg fusion, suppressed by an order of magnitude is vector boson fusion (VBF) and Higgs strahlung (VH, V=W,Z). The production in association with $t\bar{t}$ (ttH) is marginal at present energies/luminosities. The branching ratios for Higgs boson decays into gauge bosons and fermion pairs are shown on the right hand side.

Thus, searching for the Higgs boson is essentially searching for a handful of events sometimes in the presence of huge backgrounds. It is therefore imperative to check that not only QCD multijet processes are measured with enough accuracy, but also those with smaller cross-sections, like boson pair and $t\bar{t}$ production, and to check that they agree with SM predictions, as illustrated in Fig. 2.

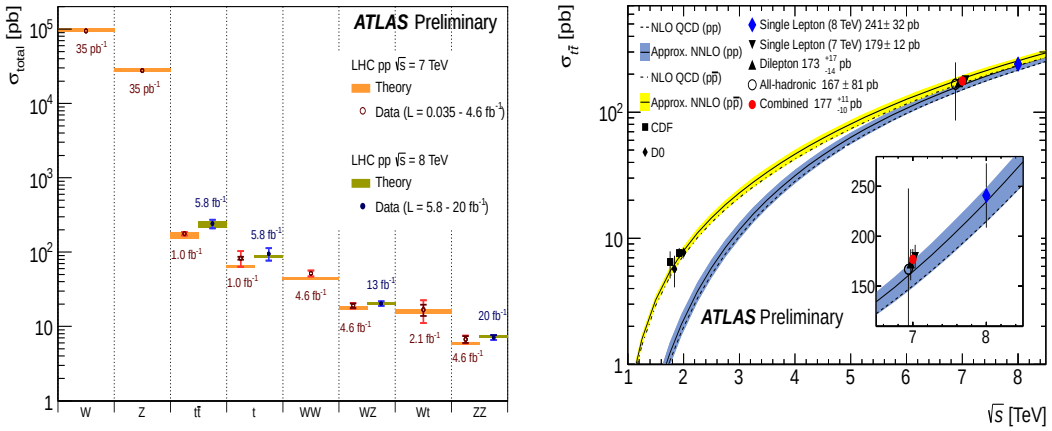

Figure 2: The cross sections for several SM processes (left) and for top production (right).

The search for Higgs has been made possible by the excellent performance of the ATLAS detector and most important the LHC machine which has delivered approximately 5 pb^{-1} at 7 TeV in 2011 and 20 pb^{-1} at 8 TeV in 2012, Fig. 3.

2 Production and couplings

It is now well over a year since the discovery of a Higgs-like particle, by the ATLAS and CMS Collaborations, was announced at CERN. At that time, July 2012, no conclusive evidence i.e. 5σ effect, had been observed in any given particular channel. The purpose of this talk is to review the progress made since then.

SM Higgs boson production processes as well as background production processes are modelled with detailed MC programmes including detector effects, as shown in Table 1, see [1] for more details.

2.1 The channel $H \to \gamma\gamma$

This channel is particularly sensitive to physics BSM since the decay proceeds via loops. Events are required to have *two isolated high* p_T *photons* with invariant mass in the range $100-160\ GeV$.

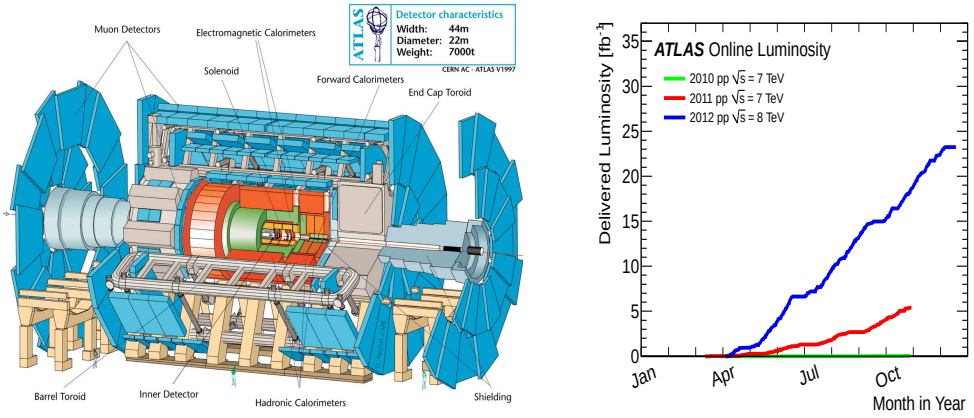

Figure 3: The ATLAS detector (left) and the delivered integrated luminosity (right).

Table 1: Event generators used to model the signal and the main background processes.

Process	Generator
ggF, VBF	POWHEG+PYTHIA
WH, ZH, $t\bar{t}H$	PYTHIA
$H \to ZZ \to 4l$ decay	PROPHECY4f
W+jets, Z/γ^*+jets	ALPGEN+HERWIG
	POWHEG+PYTHIA, SHERPA
$t\bar{t}$, tW, tb	MC@NLO+HERWIG
tqb	AcerMC+PYTHIA6
$q\bar{q} \to WW$	POWHEG+PYTHIA6
$gg \to WW$	gg2WW+HERWIG
$q\bar{q} \to ZZ^*$	POWHEG+PYTHIA
$gg \to ZZ^*$	gg2ZZ+HERWIG
WZ	MadGraph+PYTHIA6, HERWIG
$W\gamma$+jets	ALPGEN+HERWIG
$W\gamma^*$	MadGraph+PYTHIA6 for $m_{\gamma^*} < 7$ GeV
	POWHEG+PYTHIA for $m_{\gamma^*} > 7$ GeV
$q\bar{q}/gg \to \gamma\gamma$	SHERPA

The main background is continuum $\gamma\gamma$ production, with smaller contributions from $\gamma + jet$ and dijet production. The selected events are separated into 14 mutually exclusive categories in order to increase sensitivity to the overall Higgs signal as well as to specific VBF and VH production modes. This is done by demanding that the two isolated photons are accompanied by two forward jets, by leptons, E_T^{miss}, or by two low mass jets. These extra requirements are designed to enhance the sensitivity to a given production mechanism. The left hand side of Fig. 4 shows for instance how one can select VBF candidates with the help of a BDT algorithm. On the right hand side we show the photon pair invariant mass. A clear peak is observed at $m_H = 126.8 \pm 0.2(stat.) \pm 0.7(syst)\ GeV$ over a smooth background. The observed significance is 7.4σ with 4.3σ expected from the SM.

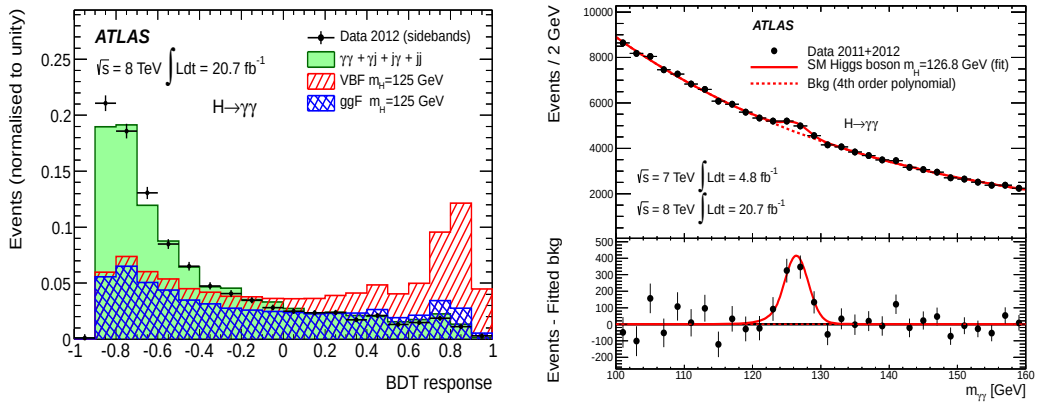

Figure 4: Selecting VBF with a BDT algorithm, left, and the diphoton invariant mass (right).

2.2 The channel $H \to 4l$

Despite the small branching ratio, this channel provides sensitivity to the Higgs coupling to Z bosons because of the large signal to background ratio. Events are required to have *two pairs of same flavour, opposite charge, high p_T isolated leptons*. The main backgrounds are ZZ^* continuum production, top pair and $Z + b\bar{b}$ production. The $4l$ invariant mass is shown on the left hand side of Fig. 5. From it one can extract $m_H = 124.3 \pm 0.6(stat.) \pm 0.5(syst.)\ GeV$. The observed significance is 6.6σ with 4.4σ expected in the SM.

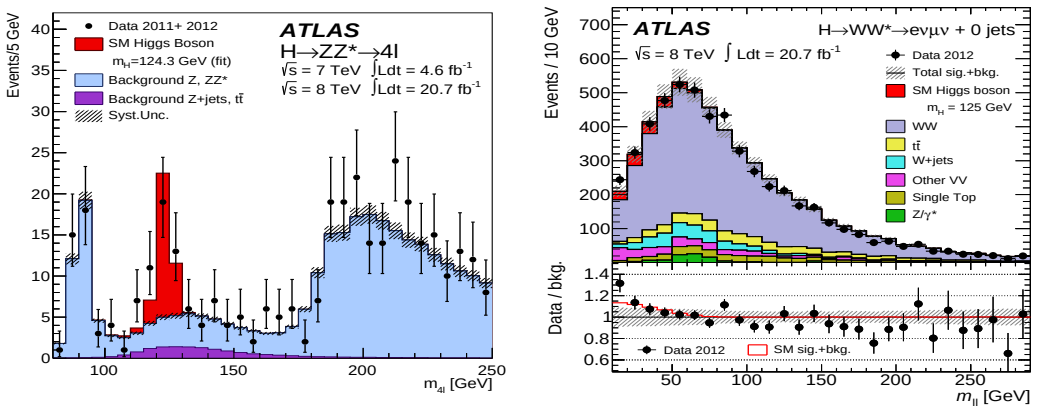

Figure 5: The distributions in m_{4l}, left, and m_{ll}, right, in the $H \to ZZ^* \to 4l$ and $H \to WW^* \to l\nu l\nu$ modes.

2.3 The channel $H \to WW^* \to l\nu l\nu$

This channel is interesting because it is sensitive to the Higgs boson coupling to W bosons. It has a large rate, but due to the production of neutrinos in the W decays, it is not possible to reconstruct the W pair invariant mass. The selection criteria require *two high p_T opposite*

charge isolated leptons plus E_T^{miss}. Dominant backgrounds are WW^* continuum production, top pair and Wt production and Drell-Yan. The selected events are classified into different categories depending on the associated jet multiplicity. The dilepton mass for $e\mu$ events with $N_{jet} = 0$ is shown on the right hand side of Fig. 5. A clear excess of events for masses below $\sim 50\ GeV$ is observed which can be attributed to $H \to WW \to e\nu\mu\nu$.

2.4 Higgs boson mass and production strengths

To derive a combined mass measurement one uses the profile likelihood method $\Lambda(m_H)$ with the individual strengths $\mu_{\gamma\gamma}$ and μ_{4l} as nuissance parameters. The combined mass is measured to be

$$m_H = 125.5 \pm 0.2\,(\text{stat})\,^{+0.5}_{-0.6}\,(\text{sys})\ \ GeV \tag{1}$$

In order to measure the production strength, μ, one uses the profile likelihood $\Lambda(\mu)$ method for the previously determined mass. The result are shown on the left hand side of Fig. 6. The overall signal production strength is:

$$\mu = 1.33 \pm 0.14\,(\text{stat}) \pm 0.15\,(\text{sys}) \tag{2}$$

To test the sensitivity to VBF production alone, the data are also fitted with $\mu_{\text{VBF}}/\mu_{\text{ggF}+ttH}$ as a free parameter, obtaining

$$\mu_{\text{VBF}}/\mu_{\text{ggF}+ttH} = 1.4^{+0.4}_{-0.3}\,(\text{stat})\,^{+0.6}_{-0.4}\,(\text{sys}) \tag{3}$$

from the combination of the three channels, see the right hand side of Fig. 6.

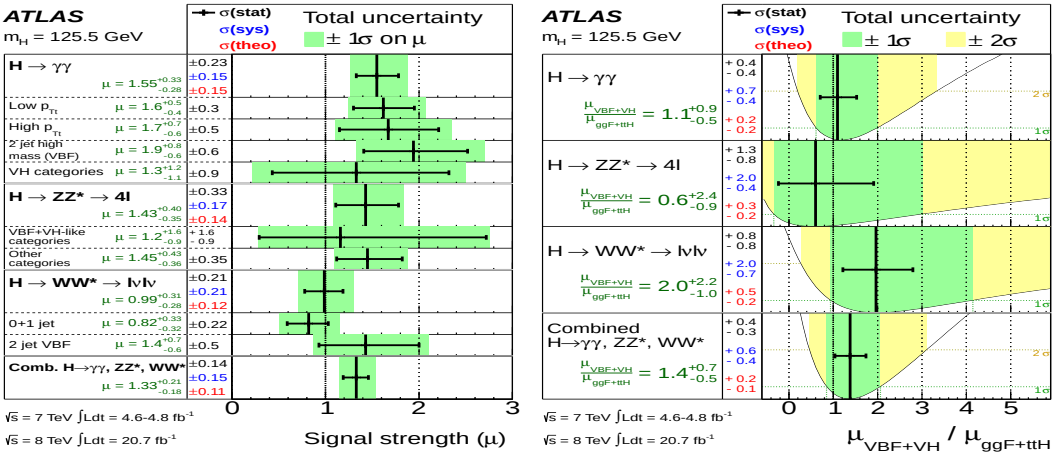

Figure 6: The fitted signal strengths for various channels.

2.5 Coupling measurements

The coupling scale factors κ_j are defined in such a way that the cross sections σ_j and the partial decay widths Γ_j associated with the SM particle j scale with κ_j^2 compared to the SM

prediction. It is assumed that the signals observed in the different channels come from a single Higgs resonance with narrow width.

Results are extracted from fits to the data using the profile likelihood ratio $\Lambda(\vec{\kappa})$, where the κ_j couplings are treated either as parameters of interest or as nuisance parameters, depending on the measurement.

The first benchmark considered here assumes one coupling scale factor for fermions, κ_F, and one for bosons, κ_V; in this scenario, the $H \to \gamma\gamma$ and $gg \to H$ loops and the total Higgs boson width depend only on κ_F and κ_V, with no contributions from physics beyond the Standard Model (BSM). The strongest constraint on κ_F comes indirectly from the $gg \to H$ production loop. The results are shown on the left hand side of fig. 7. The 68% CL intervals of κ_F and κ_V, obtained by profiling over the other parameter, are:

$$\kappa_F \in [0.76, 1.18] \quad (4)$$

$$\kappa_V \in [1.05, 1.22] \quad (5)$$

with similar contributions from the statistical and systematic uncertainties.

Many BSM physics scenarios predict the existence of new heavy particles, which can contribute to loop-induced processes such as $gg \to H$ production and $H \to \gamma\gamma$ decay. In the approach used here, it is assumed that the new particles do not contribute to the Higgs boson width and that the couplings of the known particles to the Higgs boson have SM strength (*i.e.* κ_i=1). Effective scale factors κ_g and κ_γ are introduced to parameterise the $gg \to H$ and $H \to \gamma\gamma$ loops. The results of their measurements from a fit to the data are shown on the r.h.s of Fig. 7. The best-fit values when profiling over the other parameters are:

$$\kappa_g = 1.04 \pm 0.14 \quad (6)$$

$$\kappa_\gamma = 1.20 \pm 0.15 \quad (7)$$

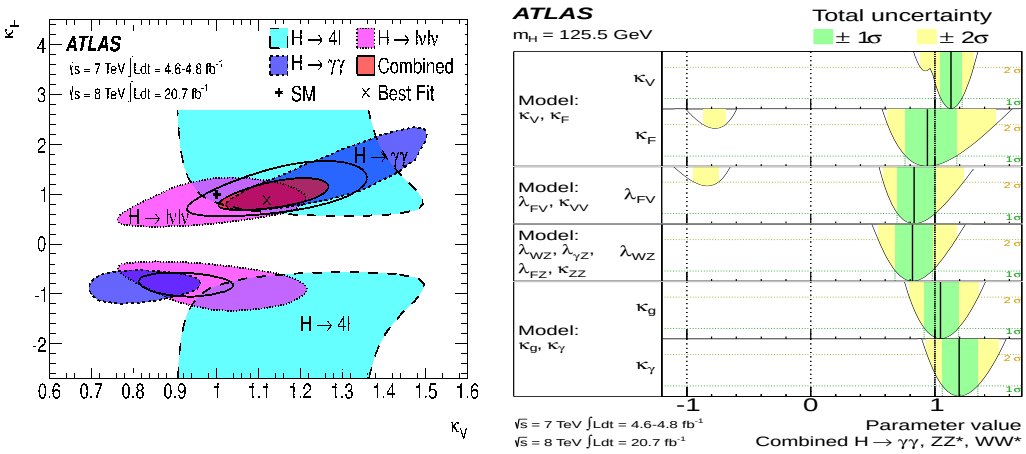

Figure 7: Determination of coupling scale factors.

3 Higgs spin-parity measurements

Evidence for the spin 0 nature of the newly discovered Higgs boson is presented in [2]. The $J^P = 0^+$ hypothesis of the SM is compared to several alternative hypotheses with $J^P = 0^-$, 1^+, 1^-, 2^+. The measurements are based on the kinematic properties of the three final states $H \to \gamma\gamma$, $H \to ZZ \to 4l$ and $H \to WW \to l\nu l\nu$. To improve the sensitivity to different spin–parity hypotheses, several final states are combined. To test the $J^P = 0^-$ spin–parity hypothesis, only the $H \to 4l$ decay mode is used, while for the $J^P = 1^+, 1^-$ hypotheses the $H \to ZZ, WW$ are combined. For the $J^P = 2^+$ study, all three decay modes are combined. A likelihood function $\mathcal{L}(J^P, \mu, \vec{\theta})$ that depends on the spin–parity assumption of the signal is constructed as a product of conditional probabilities over binned distributions of the discriminant observables in each channel:

$$\mathcal{L}(J^P, \mu, \vec{\theta}) = \prod_{j}^{N_{\text{chann.}}} \prod_{i}^{N_{\text{bins}}} P\big(N_{i,j} \mid \mu_j \cdot S_{i,j}^{(J^P)}(\vec{\theta}) + B_{i,j}(\vec{\theta})\big) \times \mathcal{A}_j(\vec{\theta}) \tag{8}$$

where μ_j represents the nuisance parameter associated with the signal rate in each channel j. The symbol $\vec{\theta}$ represents all other nuisance parameters. The likelihood function is therefore a product of Poisson distributions P corresponding to the observation of $N_{i,j}$ events in each bin i of the discriminant observable(s), given the expectations for the signal, $S_{i,j}^{(J^P)}(\vec{\theta})$, and for the background, $B_{i,j}(\vec{\theta})$. Some of the nuisance parameters are constrained by auxiliary measurements through the functions $\mathcal{A}_j(\vec{\theta})$.

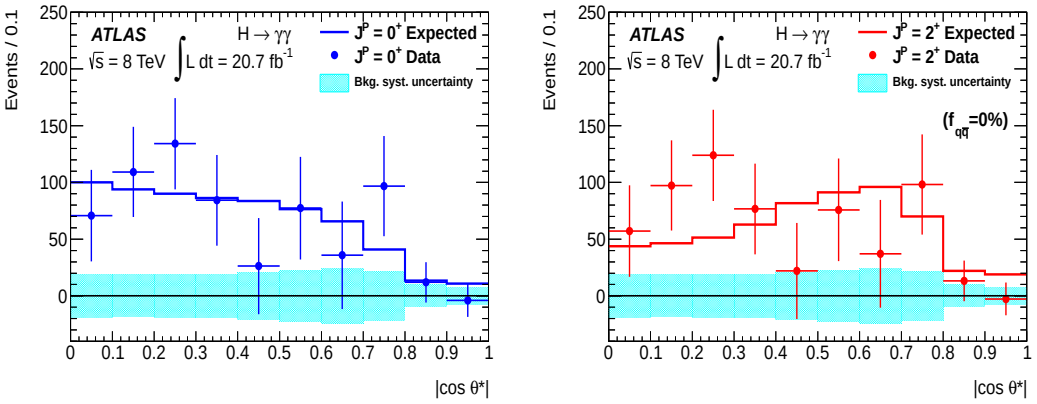

Figure 8: The background subtracted $|cos\theta^*|$ for the channel $H \to \gamma\gamma$ compared with expectations from 0^+ and 2^+ hypotheses.

The test statistic q used to distinguish between the two signal spin–parity hypotheses is based on a ratio of likelihoods:

$$q = \log \frac{\mathcal{L}(0^+, \hat{\hat{\mu}}_{0^+}, \hat{\hat{\theta}}_{0^+})}{\mathcal{L}(J^P, \hat{\hat{\mu}}_{J^P}, \hat{\hat{\theta}}_{J^P})}\,, \tag{9}$$

where $\mathcal{L}(0^+, \hat{\hat{\mu}}_{0^+}, \hat{\hat{\theta}}_{0^+})$ is the maximum likelihood estimator, evaluated under the 0^+ hypothesis and J^P stands for an alternative spin–parity assumption.

3.1 $H \to \gamma\gamma$

This decay mode is sensitive to the spin of the Higgs boson through the measurement of the polar angle distribution of the photons in the Higgs rest frame. For this channel ths SM spin hypothesis ia compared only to the $J^P = 2^+$, as shown in Fig. 8 where background subtracted distributions are presented.

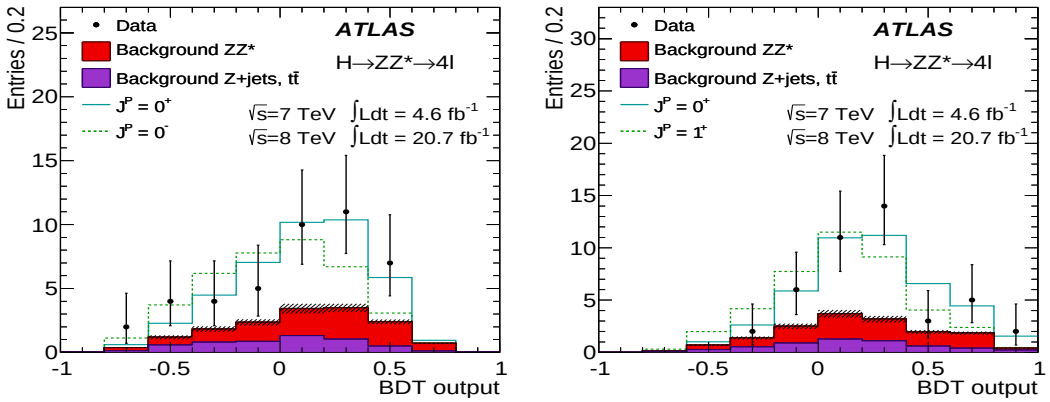

Figure 9: BDT response compared to the expectations for the SM and $J^P = 0^-, 1^+$ hypothesis.

3.2 $H \to ZZ^* \to 4l$

The two lepton pair masses as well as the five angles needed to describe the decay are fed into a BDT algorithm. The BDT response is shown in Fig. 9.

3.3 $H \to WW^* \to e\nu\mu\nu + 0 - jets$

Two variables found to be sensitive to the spin hypothesis are fed into a MVA, i.e. the lepton pair invariant mass, m_{ll} and their azimuthal separation, $\Delta\phi_{ll}$.

3.4 Summary on spin results

To illustrate the exclusion results obtained from the previous analysis we show two figures. In the left hand side of Fig. 10 we show the q distribution for the 0^+ and 0^- hypotheses from the $H \to ZZ^* \to 4l$ channel. The data, vertical black line, are in agreement with the SM and exclude the 0^- hypothesis at 97.8% CL. On the right hand side we show a summary of the exclusion limits obtained upon combining the information from all three channels.

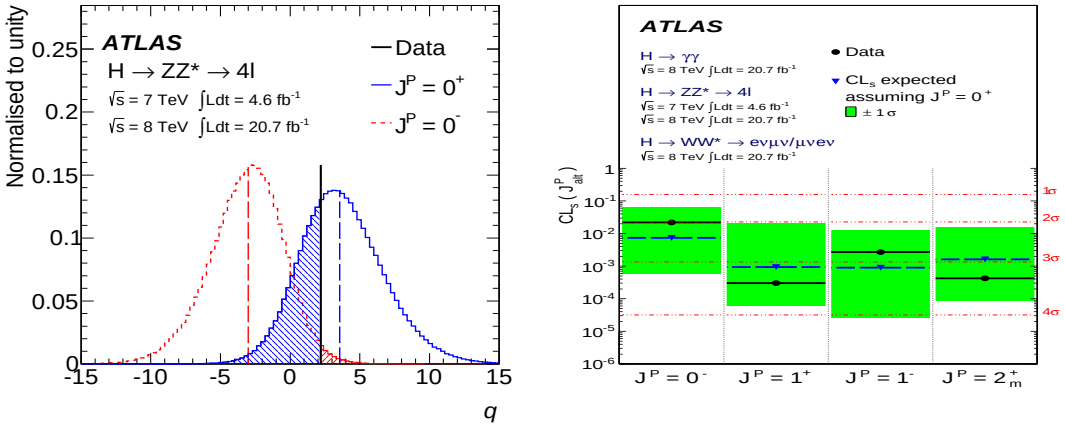

Figure 10: The q distributions for the 0^+ and 0^- hypotheses, left, and obtained exclusion limits for non SM J^P assignments, right.

4 Direct searches for Higgs decays to fermion pairs

No convincing signals have been observed yet in the decay modes $H \to \tau\tau$ and $H \to b\bar{b}$. For the latter the most promising production mechanism is Higgsstrahlung. In the l.h.s. of Fig. 11 we show the mass distribution of the $b\bar{b}$ pair, produced in association with a vector boson, with all backgrounds subtracted but for VV production. No clear signal at $\sim 125\ GeV$. The fitted production strength is, see the r.h.s. of Fig.11, $\mu = 0.2 \pm 0.5(stat) \pm 0.4(syst)\ GeV$, [3].

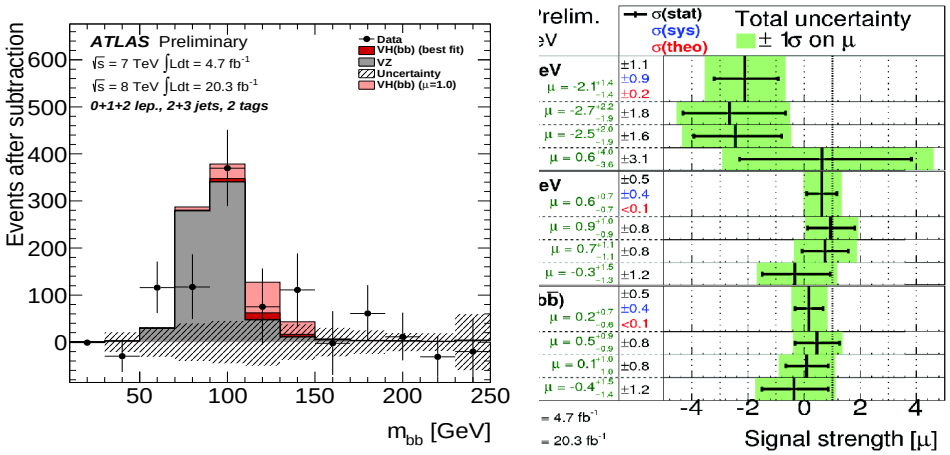

Figure 11: The background subtracted mass of the $b\bar{b}$ pair, left, and fitted production strength, right.

5 Search for charged Higgs bosons

To give a flavour of the kind of charged Higgs boson searches carried out by ATLAS, [4], we show results for light (i.e. below top quark mass) charged Higgs boson searches in the decay channel $H^+ \to c\bar{s}$. The mode is searched for in the top quark pair production channel where one top decays according to the dominant Wb mode, with the W decaying leptonically, and the second one decays via Hb. The final state consists of *one high p_T lepton, large mising transverse energy, two tagged b's and at least two high p_T additional jets.* The invariant mass of the dijet system, resulting from a kinematic fit to the full top quark pair, is shown in Fig. 12 left hand side. Good agreement with the SM is observed and limits are placed on possible H^+ signals assuming $BR(H^+ \to c\bar{s}) = 100\%$, right hand side of Fig. 12.

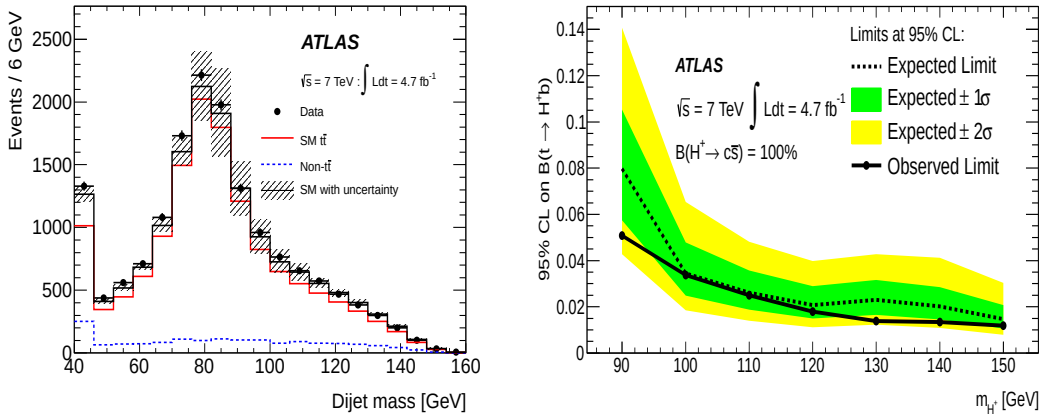

Figure 12: The dijet mass distribution for data and MC, left, and exclusion limits, right.

6 Conclusions

There is increasing evidence that the Higgs-like particle discovered a year ago, is the Higgs boson predicted in the SM. We look forward to the 14 TeV run where we will be able to reduce the uncertainties in present coupling strength measurements, find direct evidence for $H \to \tau\tau$ and/or $H \to b\bar{b}$ and put more stringent limts on possible non SM Higgses.

7 Acknowledgments

I would like to thank the local organizers for their hospitality through this superb school.

References

[1] ATLAS Coll, G. Aad *et al.*, arXiv:1307.1427[hep-ex]
[2] ATLAS Coll, G. Aad *et al.*, arXiv:1307.1432[hep-ex]
[3] ATLAS Coll, G. Aad *et al.*, ATLAS-CONF-2013-079
[4] ATLAS Coll, G. Aad *et al.*, Eur. Phys. J. **C73** (2013) 12465.